



# “Chemical Metamagnetism”: From Antiferromagnetic $\text{PrCo}_2\text{P}_2$ to Ferromagnetic $\text{Pr}_{0.8}\text{Eu}_{0.2}\text{Co}_2\text{P}_2$ via Chemical Compression

Kirill Kovnir,<sup>†</sup> William M. Reiff,<sup>†,§</sup> Alexey P. Menushenkov,<sup>||</sup> Alexander A. Yaroslavl'tsev,<sup>||</sup> Roman V. Chernikov,<sup>||,⊥</sup> and Michael Shatruk<sup>\*,†,‡</sup>

<sup>†</sup>Department of Chemistry and Biochemistry and <sup>‡</sup>National High Magnetic Field Laboratory, Florida State University, Tallahassee, Florida 32306, United States

<sup>§</sup>Department of Chemistry and Chemical Biology, Northeastern University, Boston, Massachusetts 02115, United States

<sup>||</sup>National Research Nuclear University “Moscow Engineering Physics Institute”, 115409 Moscow, Russia

<sup>⊥</sup>HASYLAB at DESY, 22603 Hamburg, Germany

**S** Supporting Information

**KEYWORDS:**  $\text{ThCr}_2\text{Si}_2$  structure type, chemical pressure, Mössbauer spectroscopy, XANES spectroscopy, mixed valence

Magnetic switching driven by external stimuli, such as temperature, pressure, or photoexcitation, is of significant fundamental and technological importance. Chemists were instrumental in creating magnetically ordered oxides and cyanides by following the fundamental orbital rules for superexchange between localized magnetic moments.<sup>1</sup> In contrast, magnetic ordering in electronically delocalized systems is dictated by the peculiarities of electronic band structure at the Fermi level.<sup>2</sup> Perhaps, this is why these so-called itinerant magnets have remained largely untapped by chemists and generally viewed as physicists' playground.<sup>3</sup> Herein we demonstrate how a rational chemical modification of an itinerant antiferromagnet allows stabilization of a ferromagnetic (FM) ground state near room temperature. Such materials can show promise for applications in sensing, data storage, and magnetic refrigeration.

In 1998, Reehuis et al. reported a fascinating pressure-induced change in the magnetic behavior of  $\text{EuCo}_2\text{P}_2$ .<sup>4</sup> Under ambient conditions, this compound exhibits an antiferromagnetic (AFM) transition at 66.5 K due to the ordering of localized  $\text{Eu}^{2+}$  magnetic moments, while the Co sublattice remains nonmagnetic. Nevertheless, under pressure above 3.1 GPa, the material develops itinerant magnetism due to the Co sublattice and shows AFM ordering at 260 K. The dramatic modification of magnetic properties was traced to the change in the oxidation state of Eu from +2 to +3, which formally leads to the electron transfer from localized Eu 4f orbitals to the Co 3d subband in the  $\text{ThCr}_2\text{Si}_2$ -type structure (Figure 1). This change is associated with a collapse of the structure along the tetragonal  $c$  axis, with the nearest P–P separation decreasing abruptly from 3.27 Å in the low-pressure (LP) phase to 2.51 Å in the high-pressure (HP) phase.<sup>5</sup>

Similar to the HP form of  $\text{EuCo}_2\text{P}_2$ , the ambient-pressure  $\text{RCo}_2\text{P}_2$  phases ( $R = \text{Ce}, \text{Pr}, \text{Nd}, \text{Sm}$ ) are characterized by the collapsed  $\text{ThCr}_2\text{Si}_2$  structure and AFM ordering of the Co sublattice above 300 K.<sup>6</sup> Only  $\text{LaCo}_2\text{P}_2$  shows a larger  $c$  axis and FM ordering at  $T_C = 132$  K.<sup>7</sup> Although it is reasonable to assume that the difference in magnetic properties originates from the strong change in the interlayer P–P distances,<sup>8</sup> from 3.16 Å in  $\text{LaCo}_2\text{P}_2$  to 2.5–2.6 Å in  $\text{RCo}_2\text{P}_2$ , we have recently shown<sup>7a</sup> that

the FM transition is sustained in  $\text{La}_{1-x}\text{Pr}_x\text{Co}_2\text{P}_2$  phases up to  $x = 0.75$ , for which  $T_C = 268$  K and  $d(\text{P}–\text{P}) = 2.67$  Å. Nevertheless, upon further decrease of the P–P distances an AFM ordering of the Co magnetic moments becomes dominant.

The delicate balance between the FM and AFM states in this family of itinerant magnets stems from the presence of a strong peak in the density of states at the Fermi level.<sup>7a</sup> This also explains why the change from  $\text{Eu}^{2+}$  to  $\text{Eu}^{3+}$  leads to the drastic modification of the magnetic behavior of  $\text{EuCo}_2\text{P}_2$ .<sup>9</sup>

The application of pressure perturbs the electronic band structure of  $\text{EuCo}_2\text{P}_2$ . Can one achieve a similar perturbation by chemical means? To answer this question, we introduced Eu into the crystal structure of  $\text{PrCo}_2\text{P}_2$ . Under ambient pressure, the volume of the coordination sphere of rare-earth ion ( $V_R$ ) is 46.39 Å<sup>3</sup> in  $\text{EuCo}_2\text{P}_2$  and 39.07 Å<sup>3</sup> in  $\text{PrCo}_2\text{P}_2$ . Hence, an  $\text{Eu}^{2+}$  ion substituted in place of a  $\text{Pr}^{3+}$  ion should experience strong chemical pressure that potentially perturbs its oxidation state. This perturbation, in turn, will influence the cooperative long-range magnetic ordering in the resulting material. Reported below are the preparation, structure, and unprecedented ferromagnetic behavior of  $\text{Pr}_{0.8}\text{Eu}_{0.2}\text{Co}_2\text{P}_2$  and its calcium analogue,  $\text{Pr}_{0.8}\text{Ca}_{0.2}\text{Co}_2\text{P}_2$ .

The synthesis of  $\text{Pr}_{0.8}\text{M}_{0.2}\text{Co}_2\text{P}_2$  ( $M = \text{Eu}, \text{Ca}$ ) was performed by annealing the starting materials in tin flux ( $\text{Pr}:\text{M}:\text{Co}:\text{P}:\text{Sn} = 0.8:0.8:2:2:30$ , total mass = 5 g) in evacuated ( $<10^{-2}$  mbar) sealed silica tubes. The mixtures were annealed at 1155 K for 10 days, cooled down to 875 at 10 K/min, and quenched into water. The Sn flux and binary rare-earth containing phases were removed by soaking the samples in dilute HCl (1:1 v/v) for 24 h. At this point, X-ray quality single crystals were selected from the samples. The elemental compositions established from energy-dispersive X-ray (EDX) analysis were close to those found from the single-crystal X-ray structure determination. No traces of Sn were detected by EDX and magnetic measurements.<sup>12</sup>

**Received:** March 17, 2011

**Revised:** May 7, 2011

**Published:** May 23, 2011

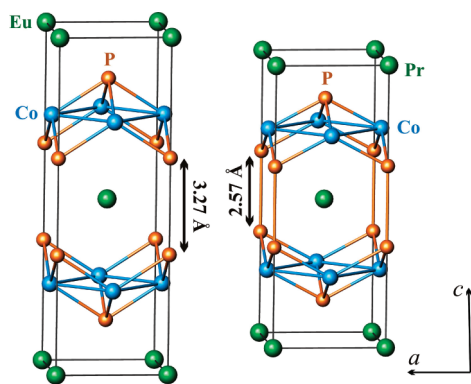


**Figure 1.** Crystal structures of  $\text{EuCo}_2\text{P}_2$ <sup>10</sup> (left) and  $\text{PrCo}_2\text{P}_2$ <sup>11</sup> (right). The interlayer P–P distances are indicated with black arrows.

**Table 1.** Crystallographic data for  $\text{ACo}_2\text{P}_2$

A	<i>a</i> , Å	<i>c</i> , Å	<i>V<sub>R</sub></i> , Å <sup>3</sup>	<i>d<sub>Co–Co</sub></i> , Å	<i>d<sub>P–P</sub></i> , Å
Eu <sup>10</sup> (LP)	3.7649	11.348	46.4	2.662	3.273
Eu <sup>5</sup> (HP)	3.856	9.651	37.9	2.727	2.511
Pr <sup>11</sup>	3.9000	9.759	39.1	2.758	2.569
Pr <sub>0.8</sub> Eu <sub>0.2</sub>	3.8994(1)	9.7972(3)	39.3(1)	2.7573(1)	2.582(3)
Pr <sub>0.8</sub> Ca <sub>0.2</sub>	3.8957(1)	9.7389(3)	38.8(2)	2.7547(1)	2.558(5)

The crystal structure of  $\text{Pr}_{0.8}\text{M}_{0.2}\text{Co}_2\text{P}_2$  (*M* = Eu, Ca) is built of alternating Pr/*M* and  $[\text{Co}_2\text{P}_2]$  layers (Figure 1). The latter is a planar square net of Co atoms, with the P atoms capping the centers of the squares above and below the plane in a chessboard-like order. The unit cell parameters of  $\text{Pr}_{0.8}\text{M}_{0.2}\text{Co}_2\text{P}_2$  are close to those of  $\text{PrCo}_2\text{P}_2$ , with volumes following the ionic radii trend:  $r(\text{Eu}^{2+}) > r(\text{Pr}^{3+}) > r(\text{Ca}^{2+})$  (Table 1). The parameter *a* and the intralayer Co–Co distance are only slightly smaller for  $\text{Pr}_{0.8}\text{M}_{0.2}\text{Co}_2\text{P}_2$  phases relative to  $\text{PrCo}_2\text{P}_2$ . Single-crystal and powder X-ray diffraction data indicate a random distribution of Pr and *M* atoms over the rare-earth crystallographic sites.

Magnetic measurements revealed that  $\text{Pr}_{0.8}\text{Eu}_{0.2}\text{Co}_2\text{P}_2$  exhibits FM ordering at  $T_C = 282(2)$  K (Figure 2), which, judging by the high Curie temperature, is attributed to the ordering of the Co sublattice. The ferromagnetic transition is rather surprising, if we recall the aforementioned antiferromagnetism of both  $\text{PrCo}_2\text{P}_2$  and the HP form of  $\text{EuCo}_2\text{P}_2$ . Even more striking is the fact that the interlayer P–P distances in  $\text{Pr}_{0.8}\text{Eu}_{0.2}\text{Co}_2\text{P}_2$ ,  $\text{PrCo}_2\text{P}_2$ , and HP- $\text{EuCo}_2\text{P}_2$  remain very similar (Table 1). Additionally, the Ca analogue,  $\text{Pr}_{0.8}\text{Ca}_{0.2}\text{Co}_2\text{P}_2$ , also shows a similarly short P–P distance and FM ordering at 278(3) K. All these observations suggest that the oxidation state of Eu in  $\text{Pr}_{0.8}\text{Eu}_{0.2}\text{Co}_2\text{P}_2$ , despite the strong compression of its crystallographic site, should be quite different from +3. Hence, incorporation of Eu into  $\text{PrCo}_2\text{P}_2$  should significantly perturb the electronic band structure.

To conclusively probe the oxidation state of Eu, a Mössbauer spectrum of  $\text{Pr}_{0.8}\text{Eu}_{0.2}\text{Co}_2\text{P}_2$  was collected at room temperature. A broad signal with  $\delta = -6.4$  mm/s (vs  $\text{EuF}_3$ ) was observed (Figure 3), which is intermediate between those found for the isostructural  $\text{EuFe}_2\text{P}_2$  at atmospheric pressure ( $\text{Eu}^{2+}$ ,  $-10.7$  mm/s) and at 12 GPa ( $\text{Eu}^{3+}$ ,  $-0.4$  mm/s).<sup>9</sup> Thus, it is more likely that Eu in  $\text{Pr}_{0.8}\text{Eu}_{0.2}\text{Co}_2\text{P}_2$  is in the intermediate oxidation state of +2.4(1).<sup>13</sup> The presence of only one such signal indicates that there is no charge ordering resulting in discrete  $\text{Eu}^{2+}$  and

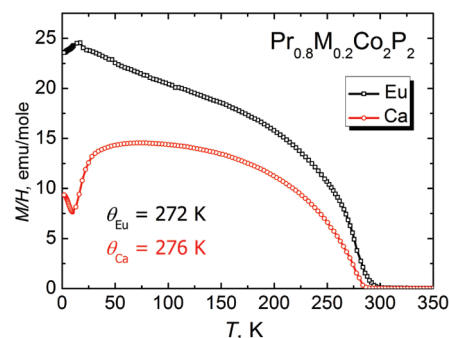


**Figure 2.** Temperature dependence of magnetic susceptibility for  $\text{Pr}_{0.8}\text{M}_{0.2}\text{Co}_2\text{P}_2$  (*M* = Eu, Ca) measured in an applied field of 0.001 T. Weiss constants are also shown for both compounds.

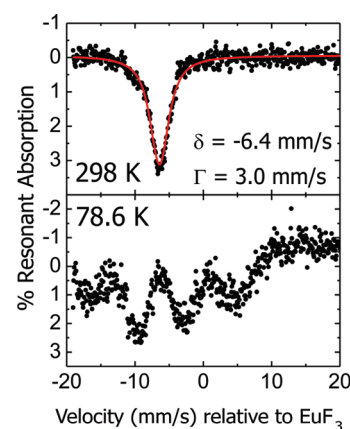


**Figure 3.** <sup>151</sup>Eu Mössbauer spectra of  $\text{Pr}_{0.8}\text{Eu}_{0.2}\text{Co}_2\text{P}_2$  at 298 and 78.6 K. The red solid line shows a Lorentzian fit.

$\text{Eu}^{3+}$  states and that the electron fluctuation rate between the localized 4f level and the conduction band is greater than the reciprocal of the excited state lifetime of the <sup>151</sup>Eu Mössbauer experiment ( $\sim 10^{-9}$  s). This is reminiscent of the situation observed in  $\text{EuNi}_2\text{P}_2$ <sup>14</sup> and  $\text{EuCu}_2\text{Si}_2$ <sup>15</sup> and clearly contrary to the behavior exhibited by so-called inhomogeneous mixed-valent systems such as  $\text{Eu}_3\text{S}_4$ <sup>16</sup> and  $\text{EuNiP}$ .<sup>17</sup>

The low-temperature Mössbauer spectrum of  $\text{Pr}_{0.8}\text{Eu}_{0.2}\text{Co}_2\text{P}_2$  collected at 78.6 K clearly exhibits magnetic hyperfine splitting (Figure 3), in accord with the ferromagnetic ordering established from magnetization measurements. The low signal-to-noise ratio is explained by the relatively high isotopic concentration of <sup>151</sup>Eu nucleus in the sample ( $\sim 4.4$  wt %) and the similar mass absorption coefficients of Pr and Eu. (See Supporting Information for more details in this context.)

Using the earlier detailed study of the isomer shift of Eu in  $\text{EuFe}_2\text{P}_2$ , which exhibits a gradual pressure-induced transition from  $\text{Eu}^{2+}$  to  $\text{Eu}^{3+}$ ,<sup>9</sup> we estimate that Eu in  $\text{Pr}_{0.8}\text{Eu}_{0.2}\text{Co}_2\text{P}_2$  experiences a strong chemical compression equivalent to  $\sim 5.6$  GPa. This is in agreement with the large difference in volumes of the  $\text{Pr}^{3+}$  and  $\text{Eu}^{2+}$  ions. Similar to the pressure-dependent behavior of  $\text{EuCo}_2\text{P}_2$ , such compression causes a partial electron transfer from  $\text{Eu}^{2+}$  to the Co 3d subband, which we estimate as  $\sim 0.1$  e<sup>−</sup> per  $\text{Pr}_{0.8}\text{Eu}_{0.2}\text{Co}_2\text{P}_2$  formula unit. Interestingly, even such small variation in the electron concentration causes the drastic modification of magnetic properties, as was postulated in our initial hypothesis.

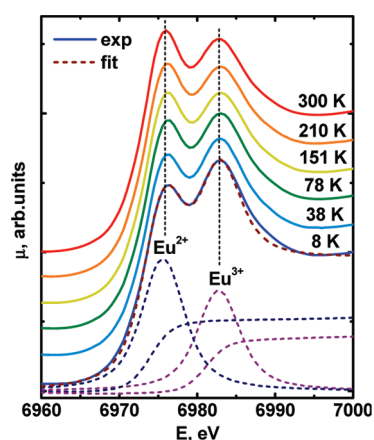


**Figure 4.**  $L_3$ -Eu XANES spectra of  $\text{Pr}_{0.8}\text{Eu}_{0.2}\text{Co}_2\text{P}_2$  at various temperatures. A fit of the 8 K spectrum with a combination of analytical functions for  $\text{Eu}^{2+}$  and  $\text{Eu}^{3+}$  contributions is shown.

X-ray absorption near edge structure (XANES) spectra of  $\text{Pr}_{0.8}\text{Eu}_{0.2}\text{Co}_2\text{P}_2$  were collected in transmission mode above the  $L_3$ -Eu (6977 eV) absorption edge. In contrast to the room-temperature Mössbauer spectrum, two absorption peaks corresponding to  $\text{Eu}^{2+}$  and  $\text{Eu}^{3+}$  are observed, similar to some other intermediate valence compounds.<sup>18</sup> The clear resolution of two maxima corresponding to different oxidation states of Eu (Figure 4) suggests that the electron fluctuation rate between the localized 4f level and the conduction band is lower than the reciprocal of excited state lifetime of XANES spectroscopy ( $\sim 10^{-15}$  s).

Upon lowering the temperature, the amplitude of  $\text{Eu}^{3+}$  peak increases while the  $\text{Eu}^{2+}$  component becomes weaker. The extraction of Eu valence components and evaluation of their contribution into the  $L_3$ -Eu XANES spectra using the conventional fitting procedure (see the Supporting Information)<sup>19</sup> revealed that the average oxidation state of Eu increases from +2.35(2) at 300 K to +2.43(2) at 8 K. The change can be explained by a gradual lattice contraction upon cooling and corresponding rise of the chemical pressure, which favors the smaller in volume  $\text{Eu}^{3+}$  state.

Density functional band structure calculations, performed using a full potential all-electron local orbital (FPLO) code,<sup>20</sup> revealed that the introduction of Eu into the  $\text{PrCo}_2\text{P}_2$  structure leads to a significant perturbation of the band structure and destabilizes the AFM state. In the AFM model of  $\text{PrCo}_2\text{P}_2$ , there are no bands crossing the Fermi level in the  $\Gamma$ -Z and X-M directions (Figure 5). This might be viewed as a stabilization factor for the AFM state. While the substitution of  $\text{Eu}^{2+}$  for  $\text{Pr}^{3+}$  has little effect on the states near the Fermi level, it does lower the position of  $E_F$  due to the donation of fewer electrons to the Co 3d subband. As a result, in the AFM model of a hypothetical compound  $\text{Pr}_{0.5}\text{Eu}_{0.5}\text{Co}_2\text{P}_2$  several bands cross the Fermi level in the  $\Gamma$ -Z and X-M directions, thus destabilizing the AFM state. Consequently, the difference in energy between the AFM and FM models of  $\text{Pr}_{0.5}\text{Eu}_{0.5}\text{Co}_2\text{P}_2$  becomes comparable to  $kT$  (Table S3 in Supporting Information).

$\text{Pr}_{0.8}\text{Eu}_{0.2}\text{Co}_2\text{P}_2$  is unique among the  $\text{RCo}_2\text{P}_2$  phases in that it exhibits an FM ordered state over a large temperature range,<sup>22</sup> despite the short interlayer P-P distance of 2.582(3) Å comparable to those found in AFM  $\text{RCo}_2\text{P}_2$  materials, including the high-pressure form of  $\text{EuCo}_2\text{P}_2$ . This points yet again to the

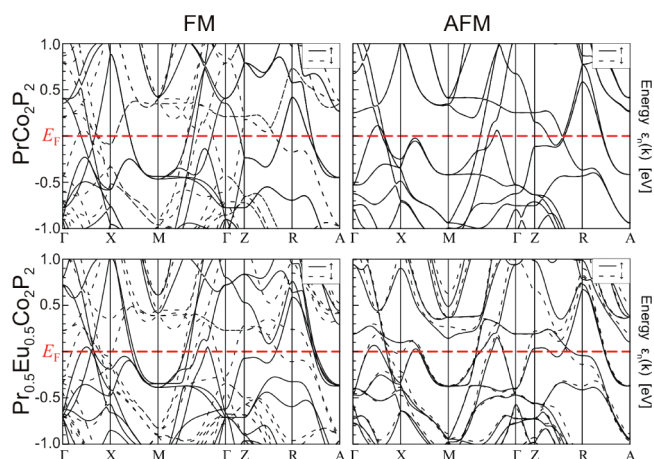


**Figure 5.** Spin-polarized band diagrams for the FM and AFM models of  $\text{PrCo}_2\text{P}_2$  and hypothetical  $\text{Pr}_{0.5}\text{Eu}_{0.5}\text{Co}_2\text{P}_2$ .

importance of electronic factors in defining the magnetic behavior of these phases. On the basis of the properties of ternary  $\text{RCo}_2\text{P}_2$  phases, one would expect that  $\text{Pr}_{0.8}\text{Eu}_{0.2}\text{Co}_2\text{P}_2$  should eventually become AFM at sufficiently high pressure, due to the stabilization of the  $\text{Eu}^{3+}$  oxidation state. Investigation of the pressure-dependent behavior of  $\text{Pr}_{0.8}\text{Eu}_{0.2}\text{Co}_2\text{P}_2$  is currently in progress, with the results to be reported in due course.

In conclusion, we have demonstrated a dramatic modification of antiferromagnetism in  $\text{PrCo}_2\text{P}_2$  upon aliovalent substitution into the Pr sublattice. Both  $\text{Pr}_{0.8}\text{Eu}_{0.2}\text{Co}_2\text{P}_2$  and  $\text{Pr}_{0.8}\text{Ca}_{0.2}\text{Co}_2\text{P}_2$  undergo a ferromagnetic phase transition due to the ordering of Co magnetic moments near 280 K. Eu in  $\text{Pr}_{0.8}\text{Eu}_{0.2}\text{Co}_2\text{P}_2$  exhibits a homogeneous mixed-valent state that is delocalized on the time scale of Mössbauer spectroscopy and not on that of XANES spectroscopy. Importantly, the change in the magnetic behavior arises not from the modification of the magnetism of the rare-earth sublattice, but from the effect the nonisoelectronic substitution in this sublattice has on delocalized band structure at the Fermi level. We believe that this approach to the control of magnetic properties by chemical means can be extended to other itinerant magnets.

## ■ ASSOCIATED CONTENT

**S Supporting Information.** Experimental procedures; additional magnetic plots; details of Mössbauer and XANES spectroscopy; and electronic structure calculations (PDF). This material is available free of charge via the Internet at <http://pubs.acs.org>.

## ■ AUTHOR INFORMATION

### Corresponding Author

\*Fax: (+1) 850-6448281. E-mail: [shatruck@chem.fsu.edu](mailto:shatruck@chem.fsu.edu).

## ■ ACKNOWLEDGMENT

M.S. acknowledges the National Science Foundation (CAREER Award DMR-0955353) for the financial support of this work. A.P.M. and A.A.Y. thank the HASYLAB Program Committee for providing beamtime.



## REFERENCES

- (1) (a) Goodenough, J. B. *Magnetism and the chemical bond*; Interscience-Wiley: New York, 1963. (b) Kanamori, J. *Prog. Theor. Phys.* **1957**, *17*, 177.
- (2) Duc, N. H.; Brommer, P. E. *Handb. Magn. Mater.* **1999**, *12*, 259.
- (3) It is becoming evident that the growth of computational power and the related improvement in our ability to perform polarized band-structure calculations open the door for chemists to investigate and modify itinerant magnets. See, for example: (a) Samolyuk, G. D.; Miller, G. M. *J. Comput. Chem.* **2008**, *29*, 2177. (b) Fokwa, B. P. T.; Lueken, H.; Dronskowski, R. *Chem.—Eur. J.* **2007**, *13*, 6040.
- (4) Cheffki, M.; Abd-Elmeguid, M. M.; Micklitz, H.; Huhnt, C.; Schlabit, W.; Reehuis, M.; Jeitschko, W. *Phys. Rev. Lett.* **1998**, *80*, 802.
- (5) Huhnt, C.; Schlabit, W.; Wurth, A.; Mewis, A.; Reehuis, M. *Phys. Rev. B* **1997**, *56*, 13796.
- (6) Reehuis, M.; Jeitschko, W. *J. Phys. Chem. Solids* **1990**, *51*, 961.
- (7) (a) Kovnir, K.; Thompson, C. M.; Zhou, H. D.; Wiebe, C. R.; Shatruk, M. *Chem. Mater.* **2010**, *22*, 1704. (b) Reehuis, M.; Ritter, C.; Ballou, R.; Jeitschko, W. *J. Magn. Magn. Mater.* **1994**, *138*, 85.
- (8) (a) Jia, S.; Williams, A. J.; Stephens, P. W.; Cava, R. J. *Phys. Rev. B* **2009**, *80*, 165107. (b) Jia, S.; Chi, S.; Lynn, J. W.; Cava, R. J. *Phys. Rev. B* **2010**, *81*, 214446. (c) Jia, S.; Cava, R. J. *Phys. Rev. B* **2010**, *82*, 180410(R). (d) Jia, S.; Jiramongkolchai, P.; Suchomel, M. R.; Toby, B. H.; Checkelsky, J. G.; Ong, N. P.; Cava, R. J. *Nat. Phys.* **2011**, *7*, 207.
- (9) Ni, B.; Abd-Elmeguid, M. M.; Micklitz, H.; Sanchez, J. P.; Vulliet, P.; Johrendt, D. *Phys. Rev. B* **2001**, *63*, 100102.
- (10) Marchand, R.; Jeitschko, W. *J. Solid State Chem.* **1978**, *24*, 351.
- (11) Jeitschko, W.; Meisen, U.; Möller, M. H.; Reehuis, M. *Z. Anorg. Allg. Chem.* **1985**, *527*, 73.
- (12) The superconducting transition in metallic tin at 3.7 K can be easily detected by magnetic measurements as the Meissner effect.
- (13) This oxidation state assignment is supported by a comparison to the isomer shifts tabulated for many Eu compounds in Grandjean, F.; Long, G. J. In *Mössbauer Spectroscopy Applied to Inorganic Chemistry*; Long, G. J., Grandjean, F., Eds.; Plenum Press: New York, 1989; Vol. 3, p 513.
- (14) (a) Perscheid, B.; Sampathkumaran, E. V.; Kaindl, G. *J. Magn. Mater.* **1985**, *47–48*, 410. (b) Bornick, R. M.; Stacy, A. M. *Chem. Mater.* **1994**, *6*, 333.
- (15) Bauminger, E. R.; Froindlich, D.; Nowik, I.; Ofer, S.; Felner, I.; Mayer, I. *Phys. Rev. Lett.* **1973**, *30*, 1053.
- (16) Röhler, J.; Kaindl, G. *Solid State Commun.* **1980**, *36*, 1055.
- (17) Ksenofontov, V.; Kandpal, H. C.; Ensling, J.; Waldeck, M.; Johrendt, D.; Mewis, A.; Gülich, P.; Felser, C. *Europhys. Lett.* **2006**, *74*, 672.
- (18) (a) Alekseev, P. A.; Mignot, J.-M.; Nemkovski, K. S.; Lazukov, V. N.; Nefedova, E. V.; Menushenkov, A. P.; Kuznetsov, A. V.; Bewley, R. I.; Gribov, A. V. *J. Exp. Theor. Phys.* **2007**, *105*, 14. (b) Yaroslavtsev, A. A.; Menushenkov, A. P.; Chernikov, R. V.; Clementiev, E. S.; Lazukov, V. N.; Zubavichus, Y. V.; Veligzhanin, A. A.; Efremova, N. N.; Gribov, A. V.; Kuchin, A. G. *Z. Kristallogr.* **2010**, *225*, 482. (c) Menushenkov, A. P.; Chernikov, R. V.; Sidorov, V. V.; Klementiev, K. V.; Alekseev, P. A.; Rybina, A. V. *J. Exp. Theor. Phys.* **2007**, *105*, 99. (d) Tsvyashchenko, A. V.; Fomicheva, L. N.; Sorokin, A. A.; Rysny, G. K.; Komissarova, B. A.; Shpinkova, L. G.; Klementiev, K. V.; Kuznetsov, A. V.; Menushenkov, A. P.; Trofimov, V. N.; Primenko, A. E.; Cortes, R. *Phys. Rev. B* **2002**, *65*, 174513.
- (19) Röhler, J. *J. Magn. Magn. Mater.* **1975**, *47–48*, 175.
- (20) Koepnik, K.; Eschrig, H. *Phys. Rev. B* **1999**, *59*, 1743. Version fplo7.00–28 within the LSDA+*U* approximation. See Supporting Information for details.
- (21) The calculation was performed for a hypothetical composition Pr<sub>0.5</sub>Eu<sub>0.5</sub>Co<sub>2</sub>P<sub>2</sub> to avoid creating a larger superstructure that would have substantially increased the calculation time. (See Supporting Information for further details.)
- (22) The maximum at 17 K in the *M/H* vs *T* curve of Pr<sub>0.8</sub>Eu<sub>0.2</sub>Co<sub>2</sub>P<sub>2</sub> (Figure 2) is due to antiferromagnetic ordering of rare-earth magnetic moments. For example, in PrCo<sub>2</sub>P<sub>2</sub> such ordering takes place at 19 K.<sup>7</sup>